Supporting Information

Growth Behavior and Interface Engineering for Photovoltaic Applications of Co-evaporated Sb_2Se_3 Thin Films on Mo Foil

Van-Quy Hoang,[a,b,‡] Sinae Park,[b,‡] Jaebaek Lee,[b] Dae-Ho Son,[b] Dae-Kue Hwang,[b] Quynh Le-Van,[a] Vo Pham Hoang Huy,[b] Se Yun Kim,[d] Kee-Jeong Yang,[b] Jin-Kyu Kang,[b] Shi-Joon Sung,[b,c,★] and Dae-Hwan Kim[b,c,★]

[a]Center for Environmental Intelligence, College of Engineering and Computer Science, VinUniversity, Gia Lam district, Hanoi 14000, Vietnam

[b]Division of Energy & Environmental Technology, DGIST, Daegu 42988, Republic of Korea

[c]Department of Interdisciplinary Engineering, DGIST, Daegu 42988, Republic of Korea

[d]Department of Advanced Materials Science & Engineering, Kyungnam University, 51767, Korea

E-mail: sjsung@dgist.ac.kr, monolith@dgist.ac.kr

†Electronic supplementary information (ESI) available. See DOI: https://doi.org/xxx

‡These authors contributed equally to this work.

Keywords: Sb_2Se_3 thin film, flexible photovoltaics, Mo foil, columnar grain growth

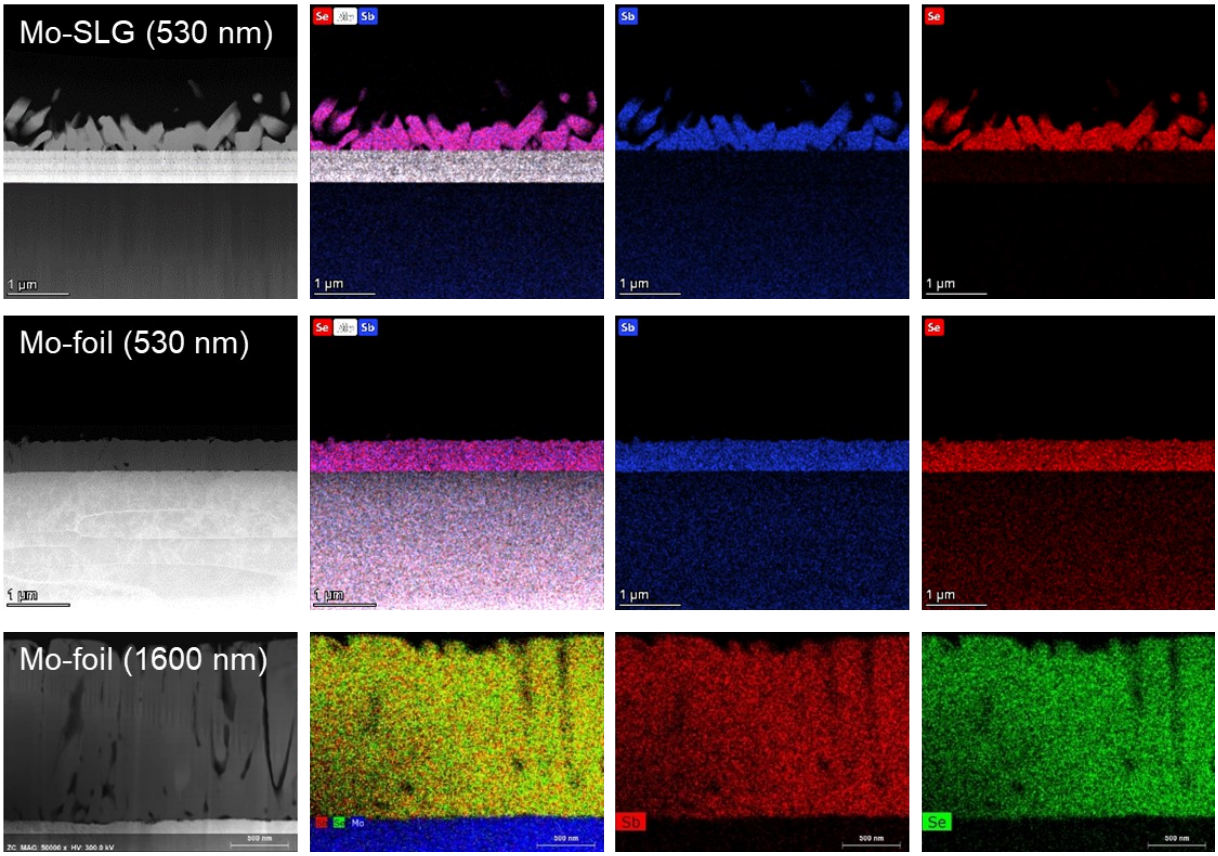

Figure S1. STEM EDS images of Sb_2Se_3 thin films on Mo or Mo-foil. For each sample, images from left to right show the cross-sectional STEM image, composite EDX elemental map, and individual elemental maps of Sb and Se.

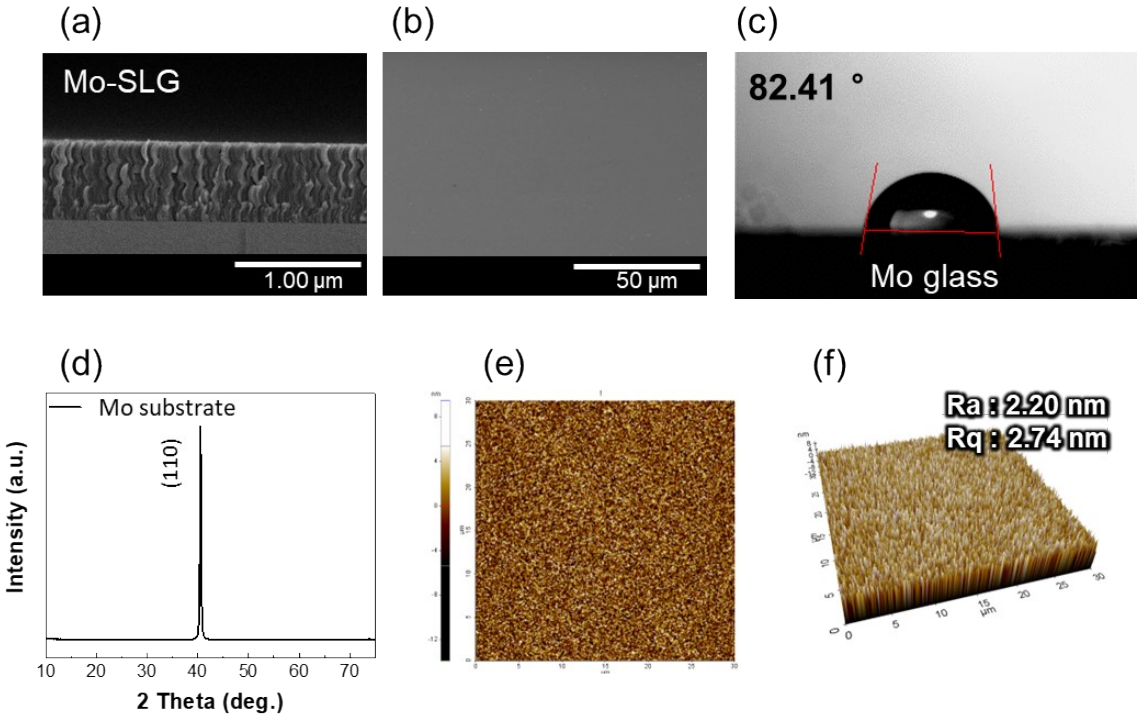

Figure S2. (a) Cross-sectional and (b) top-view SEM images of the Mo-SLG substrate, along with (c) the water contact angle measurement of the Mo-coated glass. (d) XRD and (e) AFM topography and (f) three-dimensional surface profile images, indicating a smooth Mo surface with low roughness.

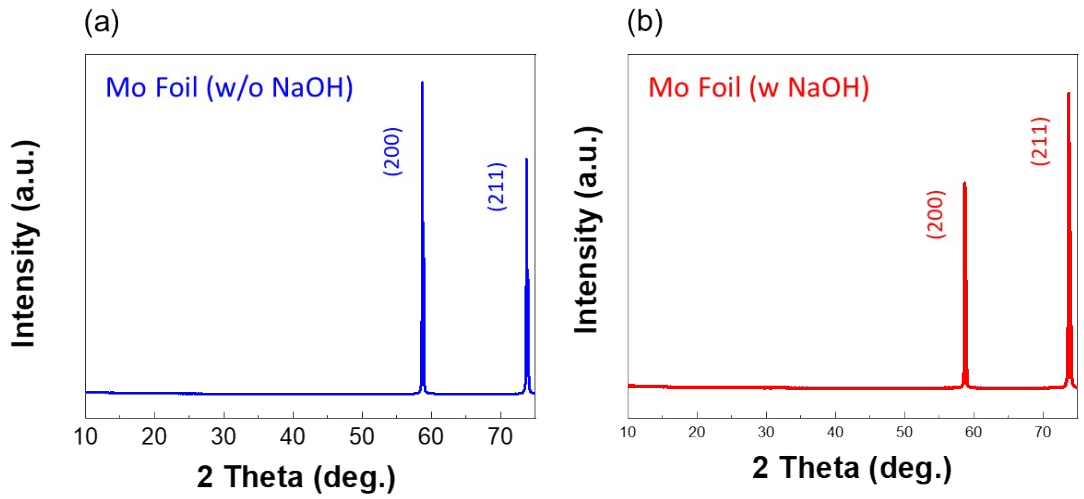

Figure S3. XRD data of Mo-foil substrates (a) without NaOH treatment (w/o NaOH) and (b) with NaOH treatment (w NaOH)

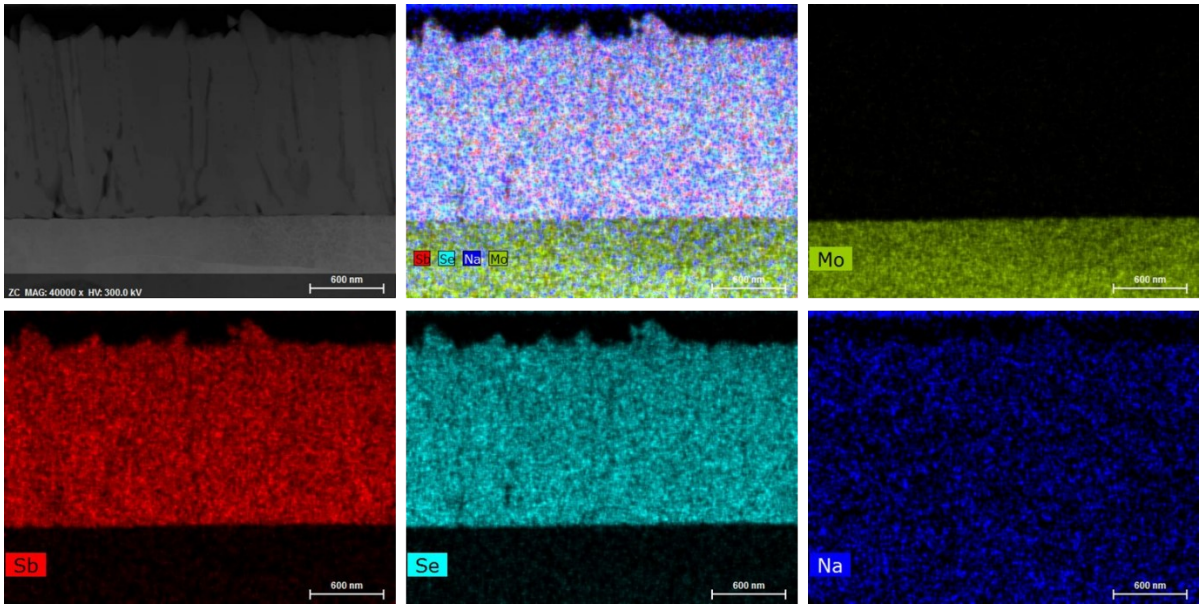

Figure S4. TEM-EDS images of 1600 nm-thick Sb_2Se_3 films on Mo-foil with NaOH treatment showing the cross-sectional STEM image, composite EDX elemental map, and individual elemental maps of Mo, Sb, Se and Na.

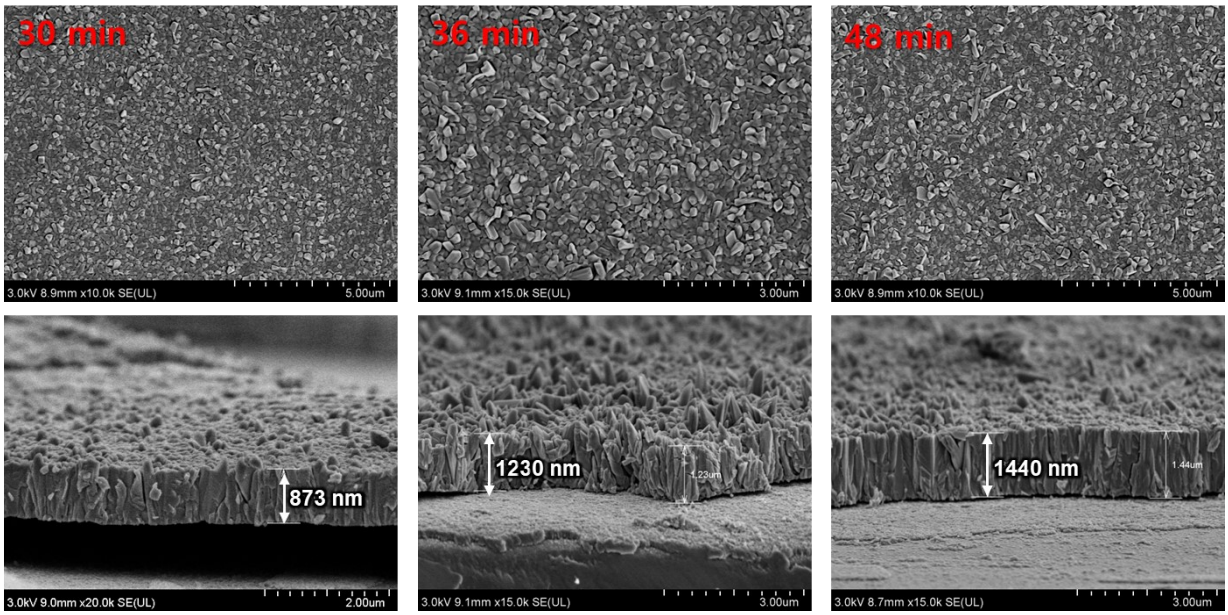

Figure S5. Top-view and cross-sectional SEM images of Sb_2Se_3 on $MoSe_2$ interlayer and NaOH treatment with different thickness from 873 nm to 1400 nm.

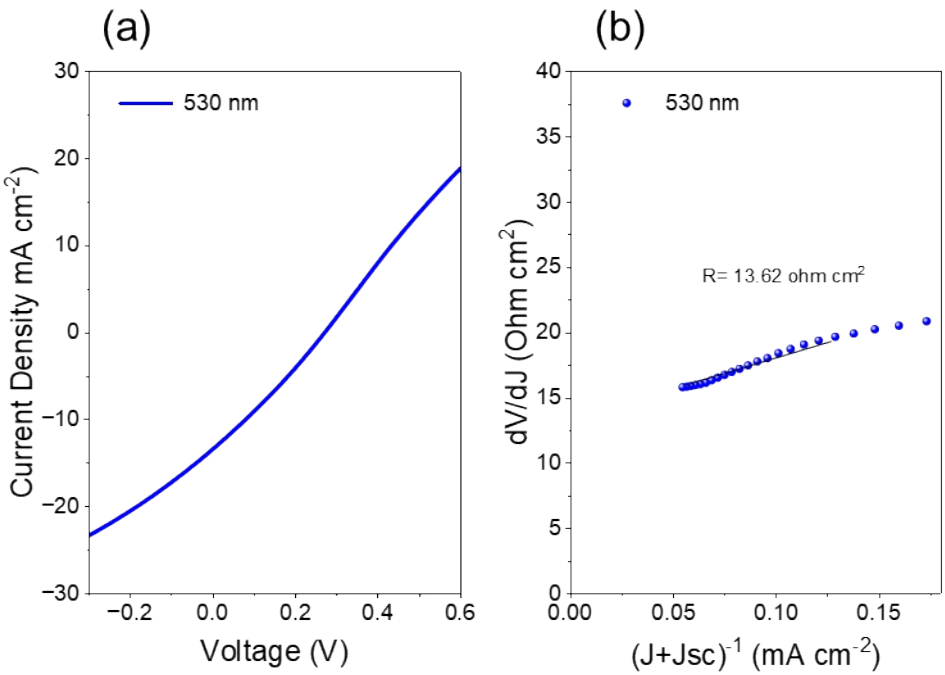

Figure S6. Characteristic behavior of the best-performing devices inclusing (a) *J*–V curves, derivative of dJ/dV for shunt characteristic analysis of 530 nm-thick Sb_2Se_3 based device.

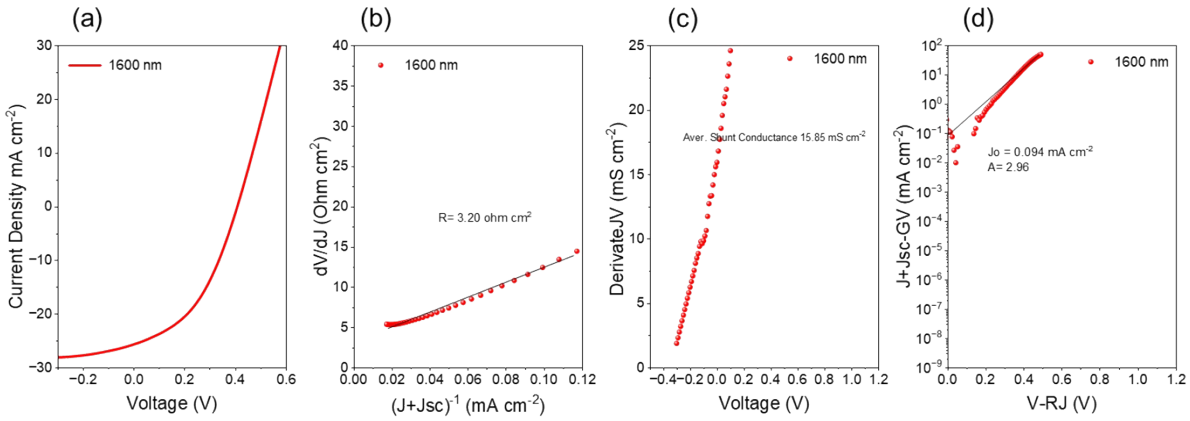

Figure S7. Characteristic behavior of the best-performing devices inclusing (a) *J*–V curves, (b) derivative of dJ/dV for shunt characteristic analysis, (c) derivatives of dV/dJ under forward bias with fitting are used to determine the series resistance and diode ideality factor and (d) ln(J + JSC − GV) versus (V − RJ)) curves of 1600 nm-thick Sb_2Se_3 based device.

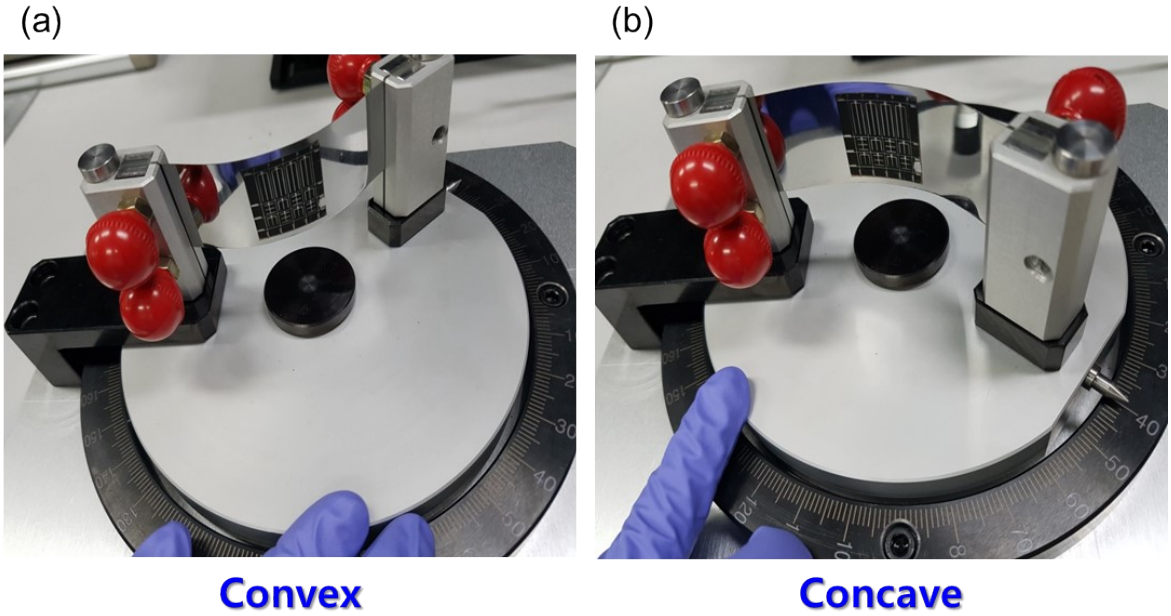

Figure S8. Experimental setups for convex (stretching) and concave (compressing) bending tests.

Table S1. Voc, J_{SC}, FF, PCE, R_s and R_{sh} of the flexible Sb_2Se_3 solar cells without and with NaOH treatment.

Treatment	V_{OC} (V)	J_{SC} (mA/cm^2)	FF (%)	PCE (%)	R_s (Ωcm^2)	R_{sh} (Ωcm^2)
w/o NaOH	0.349	19.00	44.40	2.94	6.30	100.16
w NaOH	0.341	20.27	46.65	3.23	5.60	110.75